Biomedicine & Pharmacotherapy 84 (2016) 60–70

Available online at
ScienceDirect
www.sciencedirect.com

Elsevier Masson France
EM|consulte
www.em-consulte.com/en

# Synthesis of stable nanosilver particles (AgNPs) by the proteins of seagrass *Syringodium isoetifolium* and its biomedicinal properties

N.K. Ahila[a], V. Sri Ramkumar[b], S. Prakash[a,c,*], B. Manikandan[d], J. Ravindran[d], P.K. Dhanalakshmi[e], E. Kannapiran[a,*]

[a] Department of Animal Health and Management, Science Campus, Alagappa University, Karaikudi-630 004, Tamil Nadu, India
[b] Department of Environmental Biotechnology, School of Environmental Sciences, Bharathidasan University, Tiruchirappalli-620 024, Tamil Nadu, India
[c] Department of Biotechnology, Sri Kaliswari College (Autonomous), Sivakasi-626 123, Virudhunagar, Tamilnadu, India
[d] CSIR-National Institute of Oceanography, Biological Oceanography Division, Dona Paula, Goa-403 004, India
[e] Centre for Advanced Studies in Botany, University of Madras, Maraimalai Campus, Guindy, Chennai-600 025, Tamil Nadu, India

ARTICLE INFO

*Article history:*
Received 11 June 2016
Received in revised form 29 August 2016
Accepted 1 September 2016

*Keywords:*
Seagrasses
*Syringodium isoetifolium*
Phytochrome-B
AgNPs
Antibacterial activity
Haemolysis
Cytotoxicity

ABSTRACT

A simple eco-friendly approach for the hasty synthesis of stable, potent and benign silver nanoparticles (AgNPs) using seagrass, *Syringodium isoetifolium* was proposed and described here. The UV–Vis, DLS, XRD, AFM, FESEM, EDX and HRTEM analysis highly characterized and confirmed the presence of polydispersed (2–50 nm) spherical and stable AgNPs. FT-IR and phytochemical analysis suggested that the proteins act as reducing and also as capping agent. A hypothetical approach using bioinformatics tools revealed that the Phytochrome B protein of *S. isoetifolium* might be responsible for the biosynthesis of NPs. Furthermore, biosynthesized AgNPs showed magnificent antibacterial activity against thirteen clinical bacterial pathogens with maximum zone of inhibition of $14.3 \pm 0.12$ mm due to their smaller size and longer stability even at minimal nanomolar (nM) concentration. In addition, the MIC and MBC values also suggested the same. Moreover, the percentage of haemolysis ($8.49 \pm 3.10$ to $73.34 \pm 1.79\%$) and haemolytic index revealed the satisfactory biocompatibility of AgNPs that showed less/no haemolysis up to 3 nM concentration. Further, the toxicity effect of biosynthesized AgNPs against the brine shrimp, *Artemia salina* exhibited significantly increasing mortality ($13 \pm 4.7$ to 100%) with $LC_{50}$ value at 4 nM concentration. Thus, the optical property, crystal structure, size, shape, stability, bactericidal activity, cytotoxicity, and biocompatibility apparently proved that the biologically synthesized AgNPs have typical properties of nanomaterials.



## 1. Introduction

Nanotechnology is a burgeoning interdisciplinary field combining physical, chemical and biological principles to explore the benefit of nanomaterials for the advancement of human life. They have wide applications in various fields such as biomedical, optical sensors and industries, etc. The metal nanoparticles are especially most promising due to their remarkable electromagnetic, optical, catalytic, magnetic and antibacterial properties [1]. Amongst, silver has been time-honoured as the effective antimicrobial agent that are non-toxic to humans and others [2]. Hence, it has been indiscriminately used as traditional medicine to culinary items. Therefore, the recent research advancement is to develop the experimental processes to synthesis NPs with different sizes, shapes, composition, crystallinity, controlled dispersion and improved stability. All these factors play a vital role in controlling their physical, chemical and biological properties to ameliorate their boundless applications.

Till date, a huge number of methods including physical, chemical and biological method have been developed and adopted to synthesis NPs of different size, stability and functions. The first two methods have augmented the concern of environmental conditions by generating hazardous by-products and economically expensive [3] though resulted in stable NPs. So, the need of the hour is the utilization of natural gifted sources to synthesis stable, potent and eco-friendly AgNPs for biomedical and other applications where there is no need of high pressure, energy, temperature and toxic chemicals. This greener technology is also cost effective, clean, non-toxic, has sufficient material sources and simple scaling up process. The AgNPs synthesis using biological sources like

* Corresponding authors.
*E-mail addresses:* algaprakash@gmail.com (S. Prakash), ekannapiran@gmail.com (E. Kannapiran).

http://dx.doi.org/10.1016/j.biopha.2016.09.004
0753-3322/

bacteria, actinomycetes, yeast, fungi and plants has been widely reported [4]. In particular, plants were found to be faster than microorganisms in the rate of metal ions reduction and formation of stable NPs [5]. Moreover, the size and shape of the NPs can be controlled and modulated by altering the physical conditions [6]. More advantageous in this biological method was the chemical constituents in the biological sources play a dual property as reducing agent as well as capping agent.

Furthermore, the applications of marine bionanotechnology have reached a milestone in various fields such as biomedical, food and textile technology, etc. The ocean is an untapped source of many new bioactive compounds as the environment is multifarious. Hitherto, many marine organisms and their associates were exploited for the synthesis of nanoparticles [7]. Of late, several researchers have reported various biosynthetic NPs using marine sources like seaweed [8], mangroves [9], sponges [10] and coastal medicinal plants [11]. Interestingly, literature review pointed out that the seagrasses were not fully explored for the synthesis of NPs which evoked our interest in the present study [12,13]. Among the marine resources, seagrasses are one of the highly productive and dynamic ecosystems [14]. Besides, they are the rich source of wide variety of structurally unique natural products, well known for their biomedical importance [15]. However, the seagrass, *Syringodium isoetifolium* is one of the most dominant species in the Palk Bay region with ample phytochemicals [16]. Seagrass researchers had so far investigated their biogenic potentials such as antibacterial activity against human and fish pathogens [17] and antifouling property [16,18]. Thus, with this background, the present investigation was focused to emphasize a simple, stable, hasty, cost effective, eco-friendly and efficient AgNPs with biomedical applications using aqueous extract of *S. isoetifolium*. This is the first report on virtual screening using bioinformatics tools to explore the bio-organics responsible for the bioreduction and stability.

## 2. Materials and methods

### 2.1. Preparation of seagrass aqueous extract

Seagrass samples were collected from the Palk Bay (Southeast coast of India) by hand picking at a depth of 2 m and identified as *Syringodium isoetifolium* by referring the taxonomical keys of Kuo and Hartog [19] The collected seagrass was cleaned, dried, powdered and stored for further studies. To prepare seagrass aqueous extract, one gram of seagrass powder was added in 100 ml of distilled water and boiled at 60 °C for 30 min and filtered using Whatman No.1 filter paper. The resultant filtrate was then used for the synthesis of AgNPs.

### 2.2. Biosynthesis of AgNPs

Preliminary screening was performed by blending 5 ml of aqueous *S. isoetifolium* extract to 95 ml of 1 mM silver nitrate ($AgNO_3$–Merck, India) and heated to 45 °C. The colour change from pale green to reddish brown indicates the synthesis of AgNPs. The effect of different concentrations of $AgNO_3$ (1–5 mM) in the biosynthesis of AgNPs was studied by adopting heating and incubating methods. In the heating method, the reaction was initiated by heating until a stable colour was formed whereas incubating method implies no initiation of heating and the NPs formation was monitored for 48 h at different intervals (0, 1, 6, 24, 36, 48 h). In addition, the influence of increasing concentrations of $AgNO_3$ on the stability of AgNPs was investigated up to 60 days at different intervals (1, 2, 5, 10, 30, 60 days). The kinetics of AgNPs formation was investigated at 3 mM $AgNO_3$ concentration, as the stable NPs synthesis was recorded at this concentration. The effect of pH (4–9) was also analyzed for 48 h (0, 24, 48 h). All these factors were characterized by spectral signatures of AgNPs using UV–vis spectroscopy.

### 2.3. Characterization of AgNPs

The optical property (Surface Plasmon Resonance (SPR) shift and the plasmon intensity) of the colloidal AgNPs was characterized by UV–Vis spectrophotometer (Shimadzu, Model 1800). The crystalline nature of synthesized AgNPs was analyzed by X-ray Diffraction (XRD) pattern using X' Pert PRO Analytical X-ray diffractometer with X' Pert High Score Plus Software operating at a voltage of 40 kV and current of 30 mA with Cu Kα radiation (PANalytical, Netherlands). The size and morphology of AgNPs were visualized using Field Emission Scanning Electron Microscope (FE-SEM-Hitachi SU2600, Japan) and Atomic Force Microscope (AFM-Xe 100 Park System). The purity of NPs was examined by Energy Dispersive X-ray (EDX-Horiba EMAX) spectroscopy. The size and morphology of AgNPs were further authenticated by High Resolution Transmission Electron Microscope (JEOL JEM 2100 HRTEM) operated at the accelerating voltage of 200 kV. A drop of colloidal AgNPs was coated on carbon coated copper grids of 200 mesh sizes and dried for 5 min prior to observation. In addition to this selected area electron diffraction (SAED) pattern was also performed. The size distribution of the nanoparticles in the medium was evaluated by dynamic light scattering (DLS) and particles stability was also determined by Zeta Potential (ZP) analysis (Zetasizer Ver. 6.20, Malvern Instruments, UK). Fourier Transform Infrared (FTIR-Nicolet Thermo spectrophotometer iS5, USA) spectra of seagrass aqueous extract and synthesized AgNPs colloidal mixture were analyzed in the range between 4000 and 400 $cm^{-1}$ with a resolution of 4 $cm^{-1}$ to arrive the possible functional groups responsible for reduction and capping behaviour of bio-molecules present in the aqueous seagrass extract.

### 2.4. Hypothetical approach using bioinformatics tools

A hypothetical approach was attempted to predict the protein–AgNPs interactions. A brief literature survey was made to retrieve protein sequences of *Syringodium* from Protein Data Bank of National Centre for Biotechnology Information (NCBI). The structure of obtained protein sequences were not still predicted, hence, the sequences were submitted to the Swiss model online server. Furthermore, one unit face centered cubic (fcc) silver crystal (basic unit cells of spherical NPs geometry) was docked with structure predicted protein by using Molegro Virtual Docker 5.5. The protein-metal interactions were visualized in PyMOL v1.3r1-edu, also the interaction site was confirmed with the help of FINDSITE-metal online server (Centre for the Study of Systems Biology).

### 2.5. Antibacterial properties of AgNPs

Thirteen human pathogenic bacterial strains obtained from the Microbial Type Culture Collection (MTCC), Indian Institute of Microbial Technology (IMTECH), Chandigarh, India were used to delineate the antibacterial effect of synthesized colloidal AgNPs using agar well diffusion method [16]. Pure cultures of *Streptococcus mutans, Enterococcus faecalis, Bacillus subtilis, Lactococcus lactis, Streptococcus pneumoniae*, *Staphylococcus aureus*, *Pseudomonas aeruginosa, Salmonella typhi, Escherichia coli*, *Klebsiella pneumoniae*, *Enterobacter aerogens*, *Pseudomonas putida* and *Vibrio cholerae* with a cell density of $1 \times 10^6$ cells/mL were seeded onto Mueller Hinton agar plates. The wells were loaded with different concentrations of colloidal AgNPs (20 μl–0.24 nM, 40 μl–0.48 nM, 60 μl–0.72 nM, 80 μl–0.96 nM and 100 μl–1.2 nM). After that, each plate was

incubated at room temperature for overnight. After incubation, the zone of inhibition was measured (in mm). The concentrations of colloidal AgNPs obtained from 3 mM $AgNO_3$ solution were calculated by following the method of Liu et al. [20].

To detect MIC and MBC values of AgNPs, the macrotube dilution method [16] was performed against chosen test bacterial pathogens. In brief, different concentrations of colloidal AgNPs (0.24 nM, 0.48 nM, 0.72 nM, 0.96 nM and 1.2 nM) were added to the tubes containing 0.01 ml of test pathogens with the cell density of $2 \times 10^8$ cell/ml, then the total volume was made up to 1 ml with sterile Nutrient broth and incubated at 37 °C for 24 h in a thermostat shaker. The experiments were performed in triplicate. To determine MIC and MBC, the tubes were observed for the turbidity and a loopful of each inoculum was streaked on to sterile Nutrient agar plates and again incubated at 37 °C for 24 h. The concentration which inhibits the normal growth of test pathogens was considered as MIC and concentration that ceases the growth of pathogenic bacteria was MBC.

### 2.6. Haemolysis assay

The cytotoxicity level is an important factor for any biomedical applications. Therefore, the biosynthesized AgNPs was evaluated by simple haemolysis assay following the method of Prakash et al. [21] with slight modifications. In brief, the human erythrocytes were separated from blood with 2.7% EDTA by centrifugation at 2000 rpm for 10 min and resuspended thrice in Phosphate Buffered Saline (PBS). From 10% (v/v) erythrocytes/PBS (stock), 100 μl of 1:10 diluents suspension was added to 100 μl of AgNPs at varying concentrations (0.6–15 nM). PBS and 0.1% Triton X-100 served as negative and positive controls, respectively. After 1 h of incubation at room temperature, the suspension was centrifuged and introduced into 96 well microtitre plate and the absorbance was recorded using ELISA reader at 540 nm and the percentage of haemolysis was calculated.

### 2.7. Cytotoxicity of AgNPs against Artemia salina

*Artemia* cytotoxicity assay is one of the simplest screening assays to test the toxicity of bioactive materials. The assay was conducted using 24 well plate method [16]. In brief, ten live and healthy (most active swimming) larvae of *A. salina* (I Instar) were collected from brighter portion of the hatching chamber using capillary glass tube and placed in 24 well plates containing 1 ml of sterilized seawater and various concentrations (0.6–15 nM) of AgNPs solution. Sterilized seawater without AgNPs was considered as negative control and maintained at 25 °C for 24 h under light source. After incubation, the number of larvae surviving in each test concentration was counted and the percentage of larval mortality was calculated and the 50% lethal concentration ($LC_{50}$) was determined through probit analysis. The assay was carried out in triplicate.

### 2.8. Statistical analysis

Data were expressed as mean ± SD. Results of antibacterial activity were subjected to oneway analysis of variance (ANOVA) with the SNK (Student- Newman Keuls) and *post hoc* multiple range test ($P < 0.05$) using SPSS 16.0 (Inc. Chicago, USA).

## 3. Results and discussion

### 3.1. Spectral property

Optical spectroscopy is a significant technique to authenticate the formation, kinetics, stability and morphology of NPs. In the present biosynthetic method, the AgNPs biosynthesis was preliminarily confirmed by the visual observation of prominent colour change from transparent pale green to reddish brown [10]. This is due to the excitation of Surface Plasmon Resonance (SPR), a unique optical property of metal NPs (Fig. 1) was confirmed by the UV–vis spectra. A single [22] and broad SPR band observed at 422 nm substantiates the characteristics of spherical and poly-dispersed nanoparticles, respectively in the reaction media. This was futher confirmed by several characterizations of bio-synthesized AgNPs. Compared to previous studies [23], this biosynthetic method involved very low concentration of $AgNO_3$ and also only 1% of seagrass extract which means that the aqueous biological extract composed of effective reductants. Thus, this method is simple, cheap and non-toxic which was further confirmed by haemolytic assay.

#### 3.1.1. Effect of different $AgNO_3$ concentration in the synthesis of AgNPs

Though the visible colour change was observed at 5$^{th}$ min on the mixture with the highest concentrations of $AgNO_3$ (3, 4 and 5 mM) and 10 min for 1 and 2 mM, the UV–vis spectral peak was recorded after an hour of incubation at all the studied concentrations except 1 mM where the peak was noted at 6 h of incubation. Interestingly it was noted that the spectral peak was heightened i.e., the plasmonic absorption intensity increased with increasing $AgNO_3$ concentration (Fig. S1A–E) with no significant spectral shift that clearly revealed the AgNPs synthesis increased with increasing reactant concentration and also incubation period (10 min, 1, 6, 24, 36 and 48 h) without no agglomeration.

In the heating method, a visible colour change was observed after 2 min of heating the mixture with 3, 4 and 5 mM $AgNO_3$ concentrations and after 10 min on 1 and 2 mM. After colour change of the reaction mixture, the UV–Vis spectra recorded a single narrow SPR peak of AgNPs synthesized in the range of 420–432 nm (Fig. S1 F) at different $AgNO_3$ concentrations. Similar to the incubating method, the plasmonic absorption intensity of these bands increased with increasing concentration of $AgNO_3$ with no spectral shift which obviously reflects the increased reduction rate of $Ag^+$ ions from $AgNO_3$ to $Ag^0$ and formation of AgNPs in the medium without agglomeration. In this case of increasing $AgNO_3$ concentrations, there is a chance of significant increase in the collision frequency which tends to aggregate the smaller particles to form larger particles [24]. Thus, the UV–vis spectra confirmed that the synthesis of AgNPs and size controlling were certainly

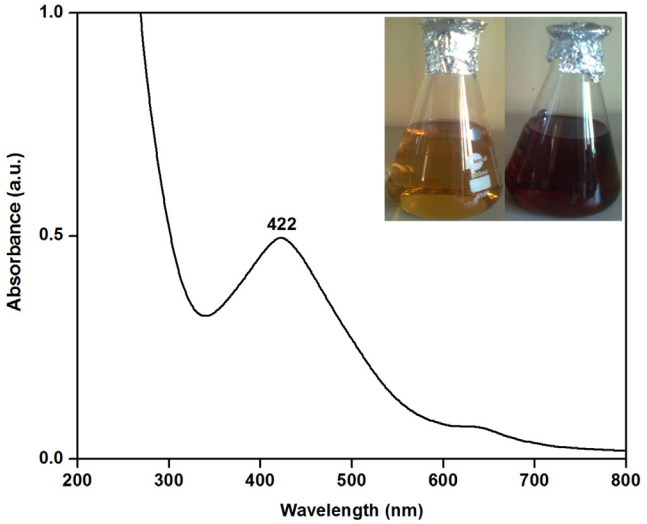


**Fig. 1.** UV–vis spectra of aqueous *S. isoetifolium* extract (Inset figure showed colour change of the reaction mixture).

dependent on the $AgNO_3$ concentration in both the synthesizing methods.

*3.1.2. Effect of different $AgNO_3$ concentration in the stability of AgNPs*

The long term interaction study of biosynthesized AgNPs colloidal solution formed by varying concentration of $AgNO_3$ was carried out for 60 days (1, 2, 5, 10, 30 and 60) to investigate their ageing effect and stability. From the absorption spectra (Fig. S2 A–F), it was clear that AgNPs synthesized using increasing $AgNO_3$ concentration stored for prolonged time gave rise to a blue shift which indicates an increase in particle size [25] with increasing $AgNO_3$ concentration (1 mM – 5 mM) with increase in the reaction time. On contrary, a red shift and broadening of SPR was observed with increase in the reaction time at all the concentrations except 3 mM. The shift towards longer wavelength and broadening of SPR may be due to decrease in the interparticle distance than their spherical dimension which results in the aggregation and alteration in spherical shape [26] with the progress of time. Moreover, the absorption peak intensity was maximum on $30^{th}$ day at all the concentrations [27] might be due to the settlement of NPs. Similar to the present study, Sathishkumar et al. [28] were also reported the stability for even 3 months after the synthesis of AgNPs using the bark extract and powder of novel *Cinnamon zeylanicum*. The above phenomenon was due to the fact that increasing $AgNO_3$ concentration with increase in days was excessive for the synthesis of AgNPs. After reaching a particular size, the reducing and capping agents cannot reduce or withhold the NP in the colloidal solution.

Interestingly, the position of SPR (429–432 nm) at 3 mM concentration remained constant throughout the study period but its intensity increased with increased reaction time which can be correlated with the higher number of NPs formation in the reaction medium. The AgNPs thus formed by this processes did not contain any aggregated particles in the solution and can be said they are quite stable. Supportively, there was no visible aggregation or flocculation of particles in the solution under light proof condition for more than six months (data not shown). This was further strongly confirmed as the observed plasmon band was symmetric when the number of days increased [29]. It may be assumed that the stability of AgNPs may be because of the negative charge due to certain bio-organic capping agents present in the aqueous seagrass extract which helps in preventing aggregation by electrostatic stabilization. The influence of $AgNO_3$ concentration and prolonged reaction time clearly pictured the formation of highly stable AgNPs at 3 mM concentration of $AgNO_3$. Thus, it is clear that the stability of NPs is also highly dependent on the concentration of $AgNO_3$ and the potency of reducing/capping agent during long time.

*3.1.3. Kinetics of AgNPs at 3 mM concentration of $AgNO_3$*

A meagre spectral shift was noticed at 429–430 nm in both the synthesizing method [30] (Fig. S3 A, B) but not significant. However, the absorption peak intensity increased with increasing incubation period from 1 to 48 h was due to the continuous formation of AgNPs in the reaction system. Prathna et al. [31] reported the AgNPs formation on 2 h using *Azadirachta indica* leaf extract and agglomeration at 4 h of interaction. Thus, the incubation method in the present study was comparably faster and no evidence of agglomeration than the previous reports of this method. Nevertheless, in the present study, the rate of bioreduction was even faster in the heating method (1 h) (Fig. S3-–B) than the incubation (2 h) (Fig. S3–A) and no agglomeration was envisioned. The mixture was heated slightly to 45 °C, to hasten the process of reduction reaction. Several reports reviewed by Firdhouse and Laitha [32] clearly evidenced that the heating method was found to be hastier than the incubating method where the latter method was mostly implied to the NPs biosynthetic methods carried out using microorganisms. It was also proved that the increasing temperature would further facilitate the biosynthesis of smaller NPs. Ibrahim [33] observed sharp narrow peaks with maximum intensity at 412 nm while heating the reaction of banana peel and $AgNO_3$ at 100 °C which indicated the synthesis of smaller Ag nanoparticles. But in the present study, the synthesis was not performed at higher temperature, as it was hypothesized that reducing compounds in the aqueous extract of *S. isoetifolium* may degrade at higher temperature, i.e., thermolabile.

Rapid bioreduction and higher intensity of AgNPs were found to be more advantageous in the heating method. Rather, Singhal et al. [34] have reported the formation of AgNPs using *Ocimum sanctum* leaf extracts within 8 min of reaction time as one of the fastest bioreducing methods to produce AgNPs at room temperature. More interestingly, the present study recorded the bioreduction of silver ions using aqueous extract of *S. isoetifolium* yielded stable NPs within 2 min of heating and 10 min of incubation. Thus, the studies clearly evidenced that these biosynthetic methods (incubating and heating) resulted in a hasty synthesis of stable AgNPs using minimal concentration of biological reducing agent and also silver nitrate.

*3.1.4. Effect of different pH in the formation of AgNPs*

A single narrow peak was observed at all the pH and reaction time (0, 24 and 48 h). A shoulder peak was noticed near 250 nm at pH 7 which may attribute to the formation of $Ag^{4+}$ clusters [35]. Amin et al. [36] have stated that at pH 4.0, there was no absorption peak in the range of 400–450 nm for the colloidal Ag suspension even after 24 h of the reaction. Conversely, in the present study a peak near 421 nm was observed at pH 4 on less than hour (Fig. S4–A).

A blue shift was observed with increase in pH of the colloidal solution (Fig. S4 A–F). Blue shift and narrow shape of SPR band indicate small and homogeneous distribution of silver NPs [35]. A red shift was also prominent with increasing reaction time. It was observed that the absorption intensity increased gradually with increase in pH, suggesting the reduction rate of Ag ions correspondingly. Similar observations have been reported by Khalil et al. [37] till pH 8 and up to pH 13 by Verma and Mehata [38]. Conversely, the precipitation was found to be increased with decreasing pH. This consequence might be because at low pH, the protein capping could have denatured and cannot withhold AgNPs. As seagrass is a marine plant, the proteins could be stable at alkaline pH and it ensures the efficient reduction and particle stability at this condition. The other reason might be more $H^+$ ions (at low pH) have more affinity towards the reducing agent, thus it could compete $AgNO_3$. Though, if NPs produced at low pH, they won't be stable. At higher pH, more $OH^-$ ions would be electrostatically repelled and hence the interaction with silver ions would be greater. It also confers that more surface negative charge supports the stability by maximizing the repulsive electrostatic/electrosteric interactions [39]. The pH of the reaction mixture has significant influence on the size [28] and shape [40] of the synthesized NPs. In the present study also, the position of SPR at different pH attributes the same. This study clearly explains that the different pH range has influence on the rate of reduction, size, shape and stability of AgNPs.

*3.2. Crystal structure and size*

The XRD pattern of AgNPs showed four characteristic 2θ peaks at 38.0°, 44.1°, 64.4° and 77.4°, respectively, indexing Bragg's reflections planes (111), (200), (220) and (311) confirmed the face-centered cubic (fcc) phase of silver (Fig. 2). Similar structure of AgNPs were synthesized using seaweed was earlier reported by

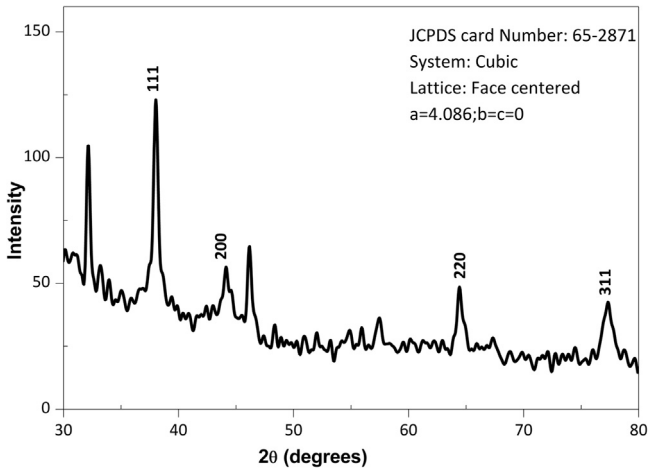


**Fig. 2.** XRD spectra of AgNPs.

Vijayan et al. [8]. The lattice constant value was calculated as $\alpha = 4.086$ A° reported by the JCPDS File No. 65-2871, which is consistent with the value of pure silver i.e., $\alpha = 4.081$ A° [41]. The average size of the Ag nanocrystallites estimated using Scherrer's formula is ~23.9 nm. It was clear that the biosynthesized AgNPs are crystalline in nature and sharpening of peaks shows that the particles are in nanoregime. Other unassigned peaks were recorded in the XRD pattern which could be originated from bio-organic molecules present in the reaction mixture for reduction and stabilization of NPs. The presence of unassigned peaks was found to be familiar in the other biosynthetic methods also [33,42].

### 3.2.1. FT-IR analysis

The FT-IR measurements showed the presence of characteristic peaks in the aqueous extract and Ag colloidal solution which revealed the dual function of biological molecules possibly responsible for the reduction and stabilization of AgNPs in the aqueous medium (Fig. 3). The characteristic peaks at 1745.96, 1634.67 and 1399.59 $cm^{-1}$ in the aqueous seagrass extract have undergone a shift to 1746.14, 1633.40 and 1384.25 $cm^{-1}$, respectively in the synthesized AgNPs (Fig. 3). The peak 1745.96 $cm^{-1}$ is attributed to the carbonyl compound (C=O) stretching and this may be due to the carboxylic acid bonding [43,44]. The peak at 1634.67 $cm^{-1}$ is assigned to amide I bonds, due to the N-H bending

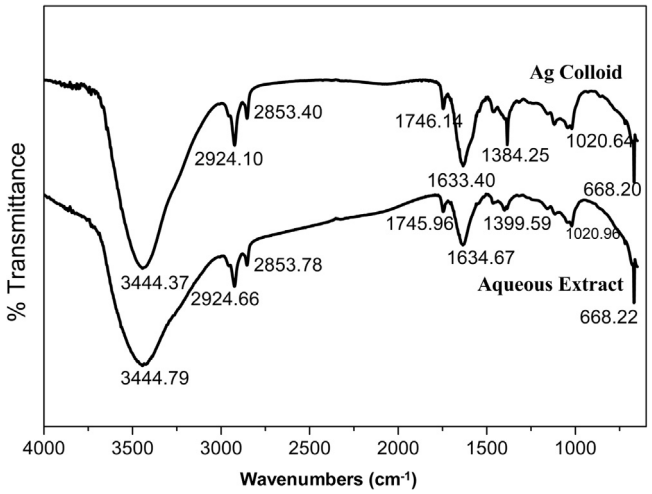


**Fig. 3.** (A) FTIR spectra of aqueous extract and (B) synthesized AgNPs.

in proteins. The more shifted band at 1399.56 $cm^{-1}$ is typical for $COO^-$ stretching vibration of amino acids [45]. It is clear that the amino groups of amino acids could have reduced ($Ag^+$ ions to $Ag^0$), and carboxylate groups have adsorbed and capped the AgNPs [46]. Thus, the IR spectroscopy study confirmed that the functional groups such as —C—C—, —C—N— and —C=C— derived from aliphatic or aromatic compounds, C=O and N—H derived from amide I bonds of amino acid residues and peptides of proteins/enzymes were responsible for the protein-NP interaction [47]. This result strongly affirms the stability of NPs characterized by their spectral property. Several researchers have described that the proteins obtained from bacteria, fungi and plants might be responsible for the possible bioreduction and capping of silver nanoparticles. The phytochemical analysis of aqueous extract of *S. isoetifolium* revealed the presence of alkaloids, flavanoids, phenols, tannins, sugars and proteins [16]. By comparing the phytochemical constituents with the FT-IR spectral studies, it was clearly understood that the amino acids in proteins were greatly responsible for the immediate bioreduction and capping of AgNPs. From this, it was clear that the proteins present in the aqueous extract of *S. isoetifolium* play a vital role in the extracellular biosynthesis of AgNPs.

### 3.2.2. Microscopic size, shape and purity

FE-SEM analysis revealed the existence of polydispersed AgNPs in the range of 10–50 nm (Fig. 4A). Due to the encapsulation of biomolecules, the edges of the particles were lighter than the centres causing them oval/elliptical in shape. Such variations in size and shape of NPs occur most commonly in biosynthesized systems [48]. We observed the property of agglomeration among NPs due to their high surface energy and surface tension. In addition, EDX analysis confirms the presence of elemental silver by sharp signals between 3 and 4 keV (Fig. 4B), which is a typical range of the optical absorption band of metallic nanocrystallites [49]. A peak between 2.5 to 2.8 keV corresponding to binding energies of Cl and AgCl might be due to the coupling reaction between any chlorine molecules in *S. isoetifolium* and elemental silver. The exact mechanism responsible for the formation of AgCl is unclear and requires further investigation. A number of spurious peaks between 0 and 2.5 keV corresponding to O, Na, Mg, Al and Si may be due to X-ray emission from proteins/enzymes present in the aqueous *S. isoetifolium* extract. The signals of S and P may correspond to protein encapsulation over elemental silver [48]. Throughout the scanning range of binding energies, no obvious peaks belonging to impurities were detected. Thus, it is apparent that the bio-synthesized product was composed of high purity AgNPs. The typical AFM analysis also confirmed the subsistence of narrow sized spherical NPs between 8 and 37 nm with the average size of 23 nm. In 2D image (Fig. 5A), the vertical distance correlates the diameter of the formed AgNPs. In 3D image (Fig. 5B), it was observed that the AgNPs are dispersed and distinctly formed.

In addition, the HRTEM provided further insight into the morphology and size of AgNPs. The synthesized AgNPs were well dispersed and no agglomeration was noticed. The uniformly small sized spherical shaped nanoparticles of the sizes ranging between 2 and 20 nm (Fig. 6A and B) were microscopically visualized. These narrow ranged sizes of nanoparticles agreed with the SPR results. The crystalline nature of AgNPs was further evidenced by the SAED pattern (Fig. 6C) with bright circular rings corresponding to Bragg's reflection planes of (111), (200), (220) and (311) [50]. The resulting SAED pattern supported the average size calculated by the XRD spectra of the present study.

### 3.2.3. Size and stability of colloidal AgNPs

The average size of the biosynthesized silver NPs was $40.15 \pm 0.31$ nm as calculated by DLS (Fig. 7A), which was greater

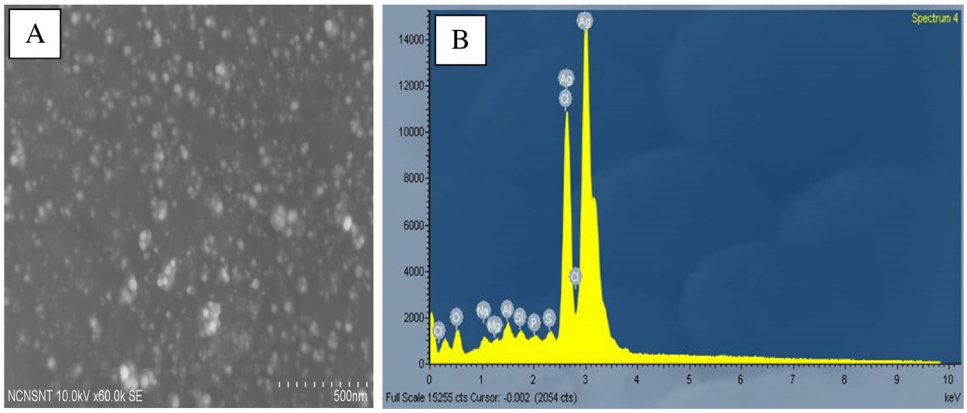


**Fig. 4.** (A) FESEM image of synthesized AgNPs and (B) EDX spectra of synthesized AgNPs.

than other instrumental calculations. Because the large particles scatter a significant amount of light (even if there is only a small amount), so the diameter given by DLS intensity distributions will be higher than other analysis [51]. In addition, the polydispersity index (pdi) confirms that the colloidal particles are hydrodynamically polydispered at a narrow range of $0.253 \pm 0.01$ [52]. A negative zeta potential value of −25 mV infers that the AgNPs are quite stable (Fig. 7B). This could be possible due to the repulsive force that exists between the NPs [53]. Also, earlier reports disclosed the presence of capping agent which plays a vital role in maintaining the stability of NPs.

### 3.3. Virtual screening of proteins

Of the total 15 amino acid sequences of *Syringodium* proteins retrieved from NCBI, Swiss model predicted 9 protein structures (Accession No. AAB93822, AEZ00156, BAJ08813, BAJ08755, BAJ08715, ADQ28379, ADQ28323, ADQ28426, ADQ28328). Among them, fcc silver crystal interacted with only one protein namely, Phytochrome B [54,55], a photoreceptor protein of *S. isoetifolium*. The Molegro Virtual Docker showed the possible dative and electrostatic interactions between the protein and silver. The Ag metal was found to be adsorbed to the 4th $\alpha$ − helix (amino acid positions from 161 to 185) portrayed in Fig. 8, where there are more hydrophobic amino acid residues such as tyrosine, phenylalanine and leucine [56]. The dative interactions of free amino groups in the basic amino acids [57] would be responsible for the reduction of $AgNO_3$. The electrostatic interaction would have formed between $COO^-$ groups and silver NPs. Hence, it can be assumed that the amino groups of arginine at the position 167 helped in the bioreduction and carboxylate groups of other amino acids in the positions 168–176 were responsible for conferring the stability by capping. This protein–metal interaction decreases with increasing size of NP cluster, as the average binding energy per atom decreases [58]. The hypothetical study emphasized the interactions between protein and metal using bioinformatics tools. Furthermore, extensive *in vitro* protein isolation, purification and structural characterization are imperative to enlighten the responsible *Syringodium* proteins involved in the metal reduction and capping.

### 3.4. Antibacterial activity

*In vitro* antibacterial activity of colloidal AgNPs showed remarkable effect against all the thirteen clinical bacterial pathogens. It was noted that the increasing concentration of colloidal AgNPs has a considerable reflection on the inhibitory activity, and the zone of inhibition (ZOI) ranged from 0 to $14.3 \pm 0.12$ mm at minimal concentration (Table 1). Out of thirteen pathogens, all the 6 Gram-positive bacteria were inhibited even at the lowest concentration (0.24 nM) whereas the maximum activity was recorded against *S. mutans* ($14.3 \pm 0.12$ mm) and minimum was against *B. subtilis* ($11.2 \pm 0.38$ mm). The inhibitory activity at the highest concentration (1.2 nM) were in the order of *S. mutans* > *E. faecalis* > *S. aureus* > *L. lactis* > *S. pneumoniae* > *B. subtilis*.

On the other hand, among seven Gram-negative bacteria, only three bacteria namely *V. cholerae* ($13.5 \pm 0.12$ mm), *P. aeruginosa* ($12.1 \pm 0.12$ mm) and *E. coli* ($11.5 \pm 0.19$ mm) were inhibited at the lowest concentration (Table 1). The antibacterial activity at the highest concentration (1.2 nM) of AgNPs were in the order of *V. cholerae* > *P. aeruginosa* > *E. coli* > *P. putida* > *K. pneumoniae* > *S. typhi* > *E. aerogens*. Rather, all the tested strains including Gram positive and negative bacteria are inhibited in the dose-dependent manner [28]. In addition, standard antibiotic drug streptomycin was also tested against these pathogens. The antibacterial activity was highly significant ($P < 0.0001$) between the bacterial pathogens and increasing AgNPs concentrations. Thus, the AgNPs synthesized using this biosynthetic method were more efficient even at low nanomolar concentration analogized to others [33,59]. This was further supported by the MIC and MBC (Table 1) values where the sensitive pathogenic bacteria were inhibited (MIC) at 0.72 nM and killed (MBC) at 0.96 nM. Rather, the more resistant bacteria such as *S. typhi*, *K. pneumoniae*, *E. aerogenes* and *P. putida* were inhibited (MIC) at the highest concentration of 1.2 nM. Several other studies have also reported MIC and MBC at various concentrations [33,59] which were comparably higher than the present study.

Most of the researchers have claimed that the antibacterial activity was more pronounced against Gram negative bacteria than Gram positive, as the cell walls possess thinner peptidoglycan layer in the former one [60,61]. The Gram positive bacteria composed of a thick layer of peptidoglycan to form a rigid structure making AgNPs difficult to penetrate. Thus, the susceptibility of Gram positive bacteria was challenging using AgNPs. Interestingly, in the present study, the antibacterial activity was comparably higher against Gram-positive bacteria than Gram-negative. Similar to the present study, Rahimi et al. [62] have reported that myco-synthesized AgNPs had more antibacterial activity against *S. aureus*, a Gram positive bacteria. The antimicrobial mechanisms of biosynthesized AgNPs may differ from species to species of target pathogenic bacteria [40]. Several mechanisms have been proposed and hypothesized to explain the antibacterial activity of AgNPs [61]. More interestingly, the metallic nanoparticles possess size and shape dependent properties in addition with stability. Undoubtedly, the bactericidal property even at the lowest concentration was influenced by its distinctive properties such

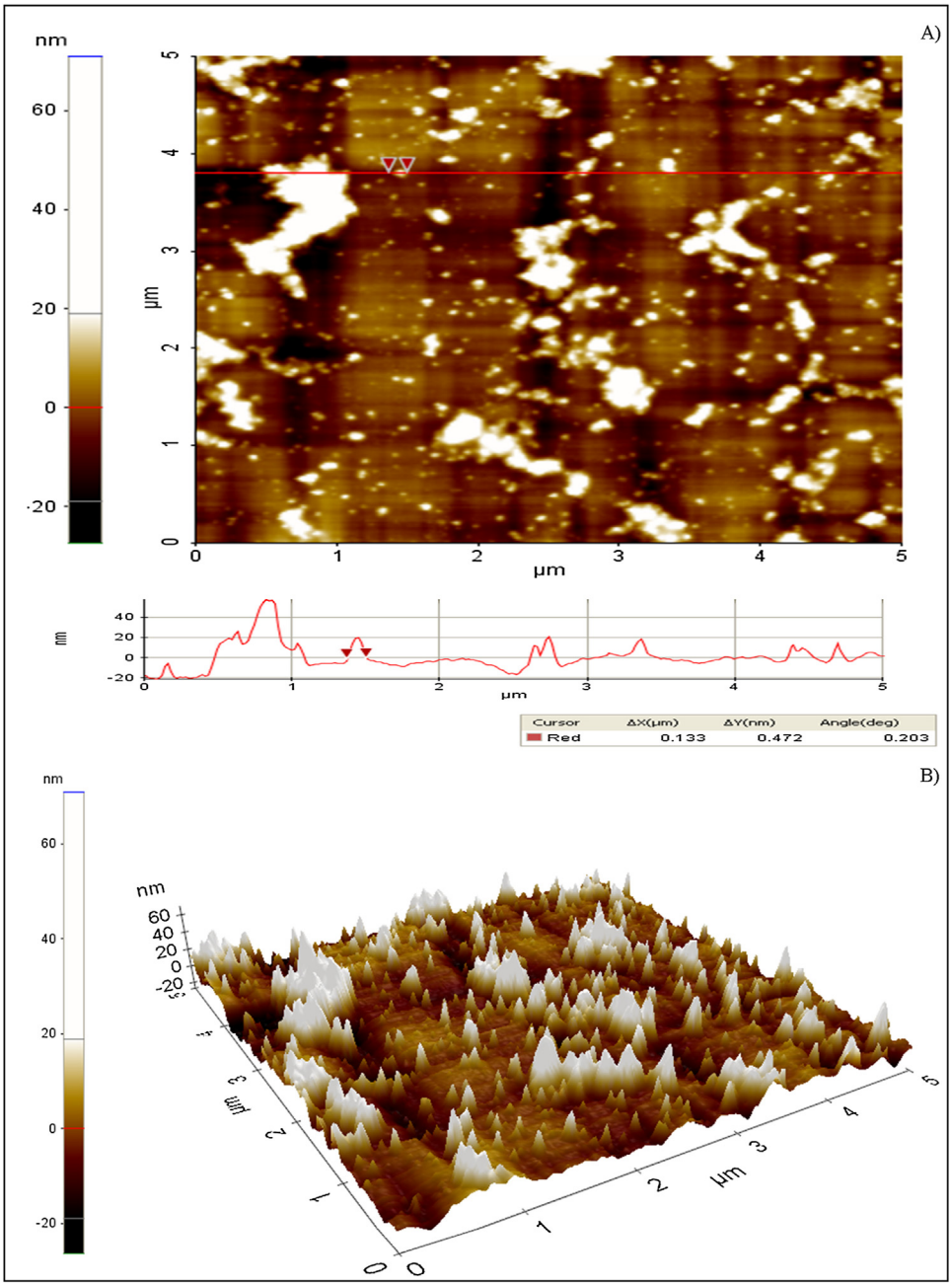


**Fig. 5.** AFM image (A) 2-D and (B) 3-D of synthesized AgNPs.

as smaller dimensions i.e., the smaller the silver nuclei, the higher the antibacterial activity, various shapes bring more interactive facets with the bacteria, chemical stability, catalytic activity and good conductivity [63] which could have lead to the increased membrane permeability and finally resulted in bacterial cell death [64]. Thus, in the present study also it can be argued that the colloidal AgNPs synthesized using the aqueous extract of *S. isoetifolium* was found to be a potent source of antibacterial agent inhibiting the growth of pathogenic bacteria might be due to their distinctive properties.

### 3.5. Haemolytic activity

The haemolytic activity of AgNPs was investigated as an indicator of its cytotoxicity to mammalian cells and also their biocompatibility. The activity was dose dependent similar to Raja et al. [65] and the maximum bactericidal concentration (1.2 nM/ml) of AgNPs caused only 14.43% lysis of erythrocytes, whereas the highest concentration of 15 nM exhibited 73% of haemolysis (Table 2). According to the standard haemolytic index, up to 3 nM AgNPs concentrations were found to be non-haemolysis, whereas high haemolysis was recorded at 9 and 15 nM concentrations. The concentration of 6 nM recorded moderate haemolysis. However, the positive control Triton-X exhibited the highest haemolytic activity over AgNPs concentrations. Several authors have reported the haemolytic activity of chemically synthesized and peptide conjugated AgNPs on human erythrocyte cells [66,67]. Nevertheless in the present study, the biosynthesized stable AgNPs remarkably exhibited low level of haemolytic activity ($P < 0.05$) at their active bactericidal nanomolar concentration. Rather, at the higher concentration, the AgNPs exhibited the cytotoxic effect. Choi et al. [68] extensively discussed the mechanisms and

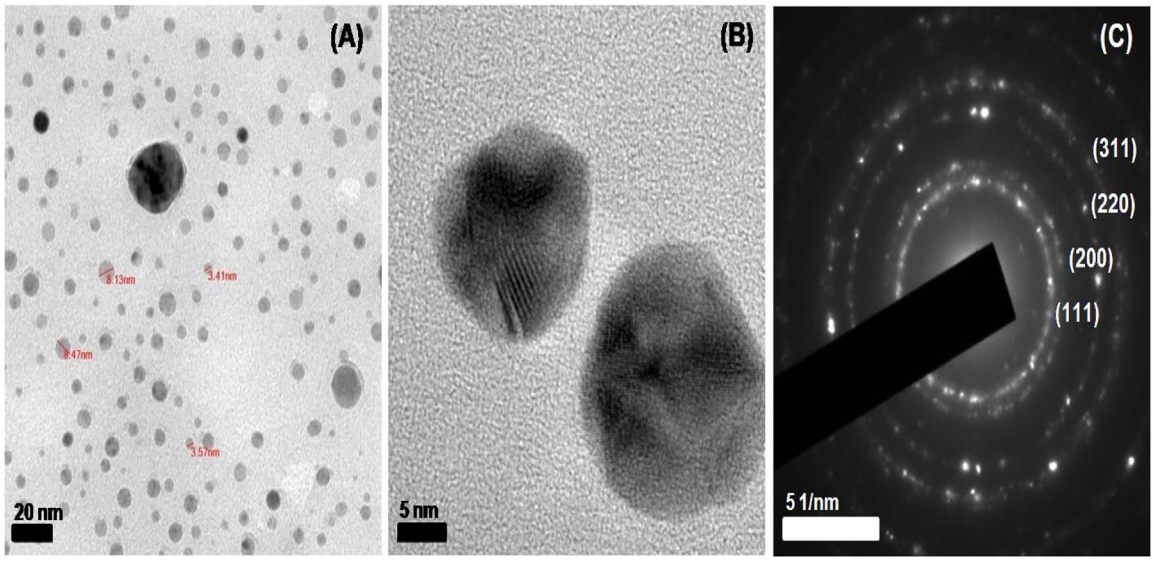


**Fig. 6.** HRTEM image (A) and (B) SAED pattern of synthesized AgNPs.

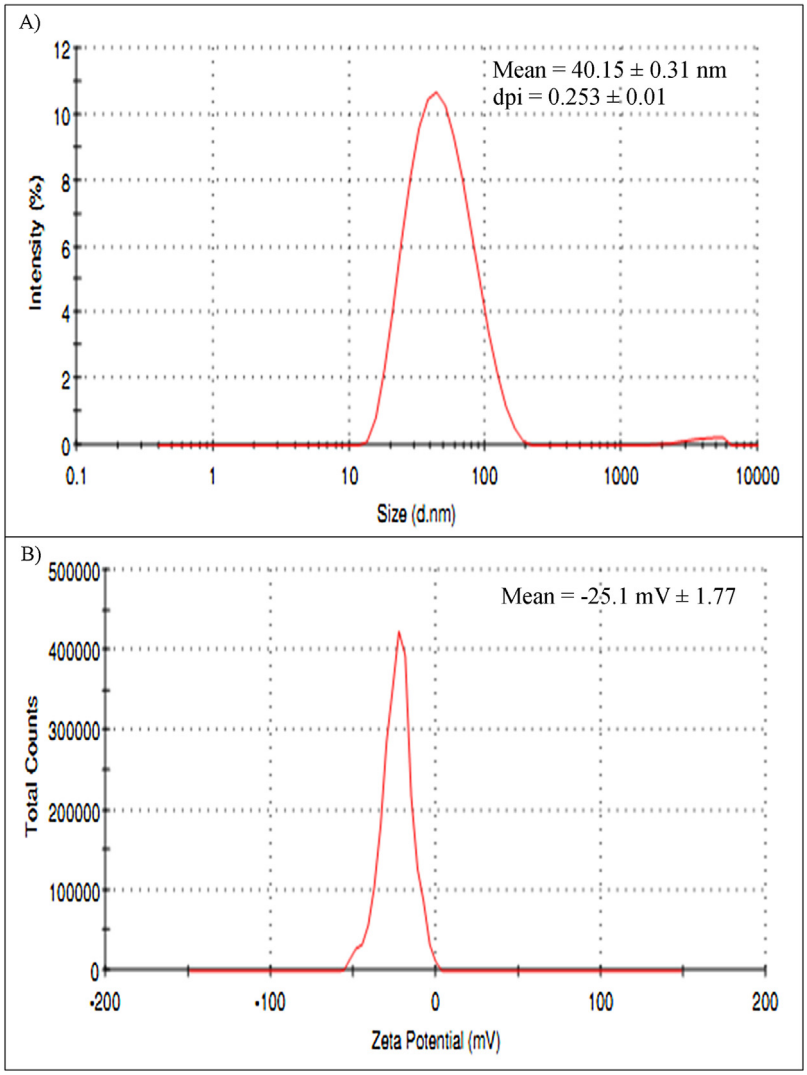


**Fig. 7.** DLS (A) Particle size distribution and (B) Zeta potential of synthesized AgNPs.

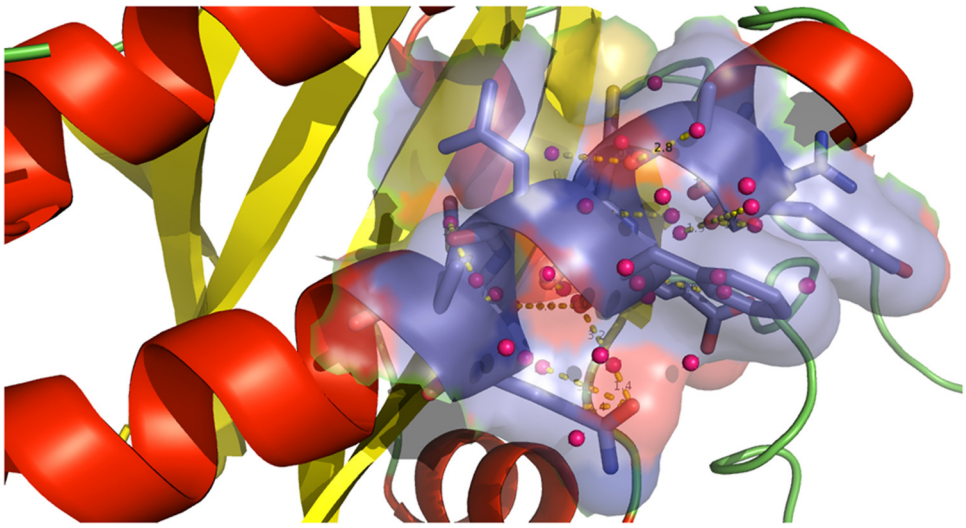


**Fig. 8.** Virtual interaction of fcc Ag with *S. isoetifolium* Phytochrome B protein [Pink colour spheres: fcc Ag atoms, blue colour surface: amino acid residues in the helix, yellow dotted line: electrostatic interaction (< 4.0 Å) between $COO^-$ (orange colour sticks) and Ag]. (For interpretation of the references to colour in this figure legend, the reader is referred to the web version of this article.)

**Table 1**
Antibacterial activity of *S. isoetifolium* synthesized AgNPs.

| Test bacterial strains | | Zone of Inhibition (mm) | MIC and MBCs of AgNPs | | | | | Streptomycin (μg/ml) | | |
|---|---|---|---|---|---|---|---|---|---|---|
| | | | Concentrations (nM) | | | | | Zone of Inhibition (mm) | MIC | MBC |
| | | | 0.24 | 0.48 | 0.72 | 0.96 | 1.2 | | | |
| *S. mutans* | Gram Positive | $14.3 \pm 0.12^{g}$ | +++ | ++ | × | | NI | $18.6 \pm 0.16^{g}$ | 3 | 5 |
| *E. faecalis* | | $13.4 \pm 0.16^{f}$ | +++ | ++ | × | | NI | $16.4 \pm 0.12^{e}$ | 5 | 7 |
| *B. subtilis* | | $11.2 \pm 0.12^{b}$ | +++ | +++ | ++ | × | NI | $19.1 \pm 0.12^{h}$ | 3 | 6 |
| *L. lactis* | | $12.4 \pm 0.21^{e}$ | +++ | ++ | × | | NI | $19.9 \pm 0.12^{i}$ | 3 | 5 |
| *S. pneumoniae* | | $12.0 \pm 0.14^{d}$ | +++ | ++ | × | | NI | $17.5 \pm 0.33^{f}$ | 5 | 8 |
| *S. aureus* | | $12.5 \pm 0.12^{e}$ | +++ | ++ | × | × | NI | $15.7 \pm 0.17^{d}$ | 5 | 6 |
| *P. aeruginosa* | Gram Negative | $12.1 \pm 0.12^{d}$ | +++ | ++ | × | × | NI | $16.7 \pm 0.26^{e}$ | 5 | 7 |
| *S. typhi* | | $0 \pm 0.0^{a}$ | +++ | +++ | +++ | ++ | × | $7.3 \pm 0.12^{b}$ | 7 | 9 |
| *E. coli* | | $11.5 \pm 0.19^{c}$ | +++ | +++ | ++ | × | NI | $16.6 \pm 0.17^{e}$ | 5 | 6 |
| *K. pneumoniae* | | $0 \pm 0.0^{a}$ | +++ | +++ | +++ | ++ | × | $7.5 \pm 0.25^{b}$ | 7 | 8 |
| *E. aerogenes* | | $0 \pm 0.0^{a}$ | +++ | +++ | +++ | ++ | × | $8.1 \pm 0.21^{c}$ | 7 | 8 |
| *P. putida* | | $0 \pm 0.0^{a}$ | +++ | +++ | +++ | ++ | × | $6.4 \pm 0.12^{a}$ | 7 | >10 |
| *V. cholerae* | | $13.5 \pm 0.12^{f}$ | +++ | ++ | × | | NI | $21.1 \pm 0.37^{j}$ | 3 | 6 |

PC: Positive control (Streptomycin–10 μg/mL); +++: Extreme growth; ++: Moderate growth; × : MIC; : MBC; NI: No Growth. Each value is the mean ± SD of three replicates value with same column with different superscripts for each group are statistically significant (One-way ANOVA test $P < 0.0001$ and subsequent *post hoc* multiple comparisons with Tukey- HSD test).

influence of AgNPs particle size and surface chemistry on haemolysis. Thus, we substantiate that the AgNPs from this biosynthetic methods were non-toxic at their bactericidal concentration, i.e., haemocompatible. Further, the cytotoxicity at higher concentration can be employed in chemotherapeutic applications with detailed investigations.

### 3.6. Cytotoxicity of AgNPs against Artemia salina

The *Artemia* cytotoxicity or anticrustacean assay is one of the reliable methods to screen and detect the toxicity of the nanomaterials. Interestingly, this is the first report on the Artemia cytotoxic activity of AgNPs synthesized using seagrass *S. isoetifolium*. The $LC_{50}$ value of the synthesized colloidal AgNPs was 3.25 nM, whereas the highest mortality of 80 and 100% were observed at 9 and 15 nM concentrations, respectively. Lethality was found to be directly proportional to the concentration of AgNPs ($P < 0.01$) (Table 2). Similar to the present study, Arulvasu et al. [69] reported the brine shrimp lethality using commercial AgNPs where $LC_{50}$ was around 10 nM and in another study, $LC_{50}$ was up to 83.57 mg/ml using green synthesized AgNPs [70]. Compared to these studies, it was clearly evident that the AgNPs synthesized using the aqueous extract of seagrass *S. isoetifolium* exhibited cytotoxicity at very low concentration of 3.25 nM of AgNPs. Thus, the biosynthesized AgNPs were cytotoxic at very least concentration could be more advantageous in the cancer treatment, also it was more effective bio-agent against *A. salina* to prevent further succession in the biofilm formation in various environment. Supportively, Prakash et al. [16] studied the anticrustacean activity using crude acetone extract of marine plants (seagrass and seaweeds) and inferred the $LC_{50}$ at 150 μg/mL. Accordingly, this study gave a cutting edge on the biomedical applications such as in cancer treatment of these nanomaterials. Further, employing bulk quantity of nanomaterials may have diverse effect in the environment, but the AgNPs from this biosynthetic method was said to be eco-friendly.

**Table 2**
Haemolytic activity and *Artemia* cytotoxicity of synthesized AgNPs of seagrass species of *S. isoetifolium*.

| Test concentrations (nM) | Haemolytic properties | | | | *Artemia salina* nauplii cytotoxicity | | |
|---|---|---|---|---|---|---|---|
| | Optical Density | Haemolysis (%) | Haemolytic index | Remarks | No. of larvae | % of mortality | $LC_{50}$ |
| 0.6 | 0.024 ± 0.002 | 8.49 ± 3.10 | 0.9 ± 0.35 | NH | 10 | 13 ± 4.7 | 4 nM |
| 1.2 | 0.030 ± 0.002 | 14.43 ± 2.31 | 1.6 ± 0.26 | NH | | 17 ± 4.7 | |
| 1.8 | 0.038 ± 0.002 | 23.68 ± 3.29 | 2.6 ± 0.37 | MH | | 37 ± 4.7 | |
| 3 | 0.045 ± 0.002 | 31.84 ± 2.70 | 3.5 ± 0.31 | MH | | 47 ± 4.7 | |
| 6 | 0.058 ± 0.001 | 45.91 ± 1.50 | 5.0 ± 0.20 | MH | | 57 ± 4.7 | |
| 9 | 0.071 ± 0.002 | 60.35 ± 2.17 | 6.6 ± 0.35 | HH | | 80 ± 8.2 | |
| 15 | 0.083 ± 0.001 | 73.31 ± 1.79 | 8.0 ± 0.25 | HH | | 100 ± 0.0 | |
| Triton-X/PC (200 μg/mL) | 0.090 ± 0.01 | 91.8 ± 1.55 | 8.8 ± 1.55 | HH | | 100 ± 0.0 | |

PC: Positive control; NH: Non-haemolysis; MH: Moderate-haemolysis; HH: High-haemolysis.

## 4. Conclusions

The biosynthetic method established using the aqueous extract of *S. isoetifolium* was simple, hastier and cost-effective which promptly biosynthesized silver nanoparticles with better optical property, reduced size, crystal structure, stability in the aqueous solution. Also, these nanostructures are the promising material with antibacterial, cytotoxic and non-toxic properties. Thus, our study provides a paradigm in developing an eco-friendly biosynthesis strategy for stable and biocompatible nanosilver were one of the advantages, and their application in various fields such as biomedical, biosensors and industrial applications. In addition, the interaction property of AgNPs with the proteins has an important implication for drug delivery systems. Furthermore, *in vivo* studies are necessary to be carried out to validate the advantages of this AgNPs.

## Acknowledgements

The authors are grateful to the authorities of Alagappa University, Karaikudi, Tamil Nadu and National Institute of Oceanography, Goa, India, for providing facilities to carry out this work. Also, Co-author (VSR) thanks University Grants Commission (UGC), New Delhi, India for the financial support through Dr. D.S. Kothari Post Doctoral Fellowship Scheme (No. F.4-2/2006 (BSR)/BL/13-14/0312, Dt.: 19th-May-2014).

## Appendix A. Supplementary data

Supplementary data associated with this article can be found, in the online version, at http://dx.doi.org/10.1016/j.biopha.2016.09.004.

## References

[1] M. Gajbhiye, J. Kesharwani, A. Ingle, A. Gade, M. Rai, Fungus-mediated synthesis of silver nanoparticles and their activity against pathogenic fungi in combination with fluconazole, Nanomed. Nanotechnol. Biol. Med. 5 (2009) 382–386.
[2] S.H. Jeong, S.Y. Yeo, S.C. Yi, The effect of filler particle size on the antibacterial properties of compounded polymer/silver fibers, J. Mater. Sci. 40 (2005) 5407–5411.
[3] V.S. Ramkumar, S. Prakash, R. Ramasubburayan, A. Pugazhendhi, K. Gopalakrishnan, E. Kannapiran, R.B. Rajendran, Seaweeds: A resource for marine bionanotechnology. Enzyme Microb. Technol. (2016), Article in press
[4] H. Korbekandi, I. Siavash, Silver nanoparticles: The delivery of nanoparticles, in: Hashim, A.A. (Ed.), InTech, 2012 (ISBN: 978-953-51-0615-9).
[5] S. Iravani, Critical review—green synthesis of metal nanoparticles using plants, Green Chem. 13 (2011) 2638–2650.
[6] I. Herrera, J.L. Gardea-Torresdey, K.L. Tiemann, J.R. Peralta-Videa, V. Armendariz, Binding of silver (I) ions by Alfalfa biomass (*Medicago sativa*): Batch pH, time, temperature, and ionic strength studies, J. Hazard. Subst. Res. 4 (2003) 1–16.
[7] N. Asmathunisha, K. Kathiresan, A review on biosynthesis of nanoparticles by marine organisms, Colloids Surf. B 103 (2013) 283–287.
[8] S.R. Vijayan, P. Santhiyagu, M. Singamuthu, N.K. Ahila, R. Jayaraman, K. Ethiraj, Synthesis and characterization of silver and gold nanoparticles using aqueous extract of seaweed, *Turbinaria conoides*, and their antimicrofouling activity, Sci. World J. (2014) e938272.
[9] M. Gnanadesigan, M. Anand, S. Ravikumar, M. Maruthupandy, M. Syed Ali, V. Vijayakumar, A.K. Kumaraguru, Antibacterial potential of biosynthesized silver nanoparticles using *Avicennia marina* mangrove plant, Appl. Nanosci. 2 (2011) 143–147.
[10] D. Inbakandan, R. Venkatesan, S. Ajmal Khan, Biosynthesis of gold nanoparticles utilizing marine sponge *Acanthella elongata* (Dendy, 1905), Colloids Surf. B 81 (2010) 634–639.
[11] K. Kathiresan, N.M. Alikunhi, A. Nabikhan, *In vitro* synthesis of antimicrobial silver nanoparticles by mangroves: saltmarshes and plants of coastal origin, Int. J. Biomed. Nanosci. Nanotechnol. 2 (2012) 284–298.
[12] A.B. Chanthini, G. Balasubramani, R. Ramkumar, R. Sowmiya, M.D. Balakumaran, P.T. Kalaichelvan, P. Perumal, Structural characterization antioxidant and *in vitro* cytotoxic properties of seagrass, *Cymodocea serrulata* (R. Br.) Asch. & Magnus mediated silver nanoparticles, J. Photochem. Photobiol. B 153 (2015) 145–152.
[13] P. Palaniappan, G. Sathishkumar, R. Sankar, Fabrication of nano-silver particles using *Cymodocea serrulata* and its cytotoxicity effect against human lung cancer A549 cells line, Spectrochim. Acta A 138 (2015) 885–890.
[14] C.P. McRoy, C. McMillan, Production ecology and physiology of seagrasses, in: P.C. McRoy, C. Helfferich (Eds.), Seagrass Ecosystems: A scientific perspective, Marcel Dekker, New York, 1977, pp. 263–293.
[15] R.R.R. Kannan, R. Arumugam, P. Iyapparaj, T. Thangaradjou, P. Anantharaman, *In vitro* antibacterial, cytotoxicity and haemolytic activities and phytochemical analysis of seagrasses from the Gulf of Mannar, South India, Food Chem. 136 (2013) 1484–1489.
[16] S. Prakash, N.K. Ahila, V. Sri Ramkumar, J. Ravindran, E. Kannapiran, Antimicrofouling properties of chosen marine plants: an eco-friendly approach to restrain marine microfoulers, Biocatal. Agric. Biotechnol. 4 (2015) 114–121.
[17] S. Ravikumar, R. Vinoth, G. Palaniselvan, Bioactive potential of a seagrass *Syringodium isoetifolium* against bacterial fish pathogens, J. Pharm. Res. 4 (2011) 1854–1856.
[18] P. Iyapparaj, P. Revathi, R. Ramasubburayan, S. Prakash, P. Anantharaman, G. Immanuel, A. Palavesam, Antifouling activity of the methanolic extract of *Syringodium isoetifolium*: and its toxicity relative to tributyltin on the ovarian development of brown mussel *Perna indica*, Ecotox. Environ. Safe. 89 (2013) 231–238.
[19] J. Kuo, C.D. Hartog, Seagrass taxonomy and identification key, in: F.T. Short, R.G. Coles (Eds.), Global Seagrass Research Methods, Elsevier Science, B.V Amsterdam, 2001, pp. 31–58.
[20] X. Liu, M. Atwater, J. Wang, Q. Huo, Extinction coefficient of gold nanoparticles with different sizes and different capping ligands, Colloids Surf. B 58 (2007) 3–7.
[21] S. Prakash, R. Ramasubburayan, V.S. Ramkumar, E. Kannapiran, A. Palavesam, G. Immanuel, *In vitro* – Scientific evaluation on antimicrobial antioxidant, cytotoxic properties and phytochemical constituents of traditional coastal medicinal plants, Biomed. Pharmacotherapy 83 (2016) 648–657.
[22] G. Mie, Beiträge zur optik trüber medien, Ann. Phys. 25 (1908) 374–445.
[23] C. Mohandass, A.S. Vijayaraj, R. Rajasabapathy, S. Satheeshbabu, S.V. Rao, C. Shiva, I. De-Mello, Biosynthesis of silver nanoparticles from marine seaweed *Sargassum cinereum* and their antibacterial activity, Indian J. Pharm. Sci. 75 (2013) 606–610.
[24] D.K. Bhui, H. Bar, P. Sarkar, G.P. Sahoo, S.P. De, A. Misra, Synthesis and UV–vis spectroscopic study of silver nanoparticles in aqueous SDS solution, J. Mol. Liq. 145 (2009) 33–37.
[25] W. Zhang, X. Qiao, J. Chen, Formation of silver nanoparticles in SDS inverse microemulsions, Mater. Chem. Phys. 109 (2008) 411–416.
[26] D.D. Evanoff Jr., G. Chumanov, Synthesis and optical properties of silver nanoparticles and arrays, Chem. Phys. Chem. 6 (2005) 1221–1231.
[27] A. Tripathy, M.A. Raichur, N. Chandrasekaran, T.C. Prathna, A. Mukherjee, Process variables in biomimetic synthesis of silver nanoparticles by aqueous

extract of *Azadirachta indica* (Neem) leaves, J. Nanopart. Res. 12 (2010) 237–246.
[28] M. Sathishkumar, K. Sneha, S.W. Won, C.-W. Cho, S. Kim, Y.-S. Yun, *Cinnamon zeylanicum* bark extract and powder mediated green synthesis of nano-crystalline silver particles and its bactericidal activity, Colloids Surf. B 73 (2009) 332–338.
[29] S. Ponarulselvam, C. Panneerselvam, K. Murugan, N. Aarthi, K. Kalimuthu, S. Thangamani, Synthesis of silver nanoparticles using leaves of *Catharanthus roseus* Linn. G. Don and their antiplasmodial activities, Asian Pac. J. Trop. Biomed. 2 (2012) 574–580.
[30] A. Bankar, B. Joshi, A.R. Kumar, S. Zinjarde, Banana peel extract mediated novel route for the synthesis of silver nanoparticles, Colloids Surf. A 368 (2010) 58–63.
[31] T.C. Prathna, N. Chandrasekaran, A.M. Raichur, A. Mukherjee, Kinetic evolution studies of silver nanoparticles in a bio-based green synthesis process, Colloids Surf. A 377 (2011) 212–216.
[32] M.J. Firdhouse, P. Laitha, Biosynthesis of silver nanoparticles and its applications, J. Nanotechnol. 2015 (2015) 18 (Article ID 829526, 18 pages).
[33] H.M.M. Ibrahim, Green synthesis and characterization of silver nanoparticles using banana peel extract and their antimicrobial activity against representative microorganisms, J. Radiat. Res. Appl. Sci. 8 (2015) 265–275.
[34] G. Singhal, R. Bhavesh, K. Kasariya, A.R. Sharma, R.P. Singh, Biosynthesis of silver nanoparticles using *Ocimum sanctum* (Tulsi) leaf extract and screening its antimicrobial activity, J. Nanopart. Res. 13 (2011) 2981–2988.
[35] C. Petit, P. Lixon, M.P. Pileni, *In situ* synthesis of silver nanocluster in AOT reverse micelles, J. Phys. Chem. 97 (1993) 12974–12983.
[36] M. Amin, F. Anwar, M.R. Janjua, M.A. Iqbal, U. Rashid, Green synthesis of silver nanoparticles through reduction with *Solanum xanthocarpum* L. Berry extract: characterization: antimicrobial and urease inhibitory activities against *Helicobacter pylori*, Int. J. Mol. Sci. 13 (2012) 9923–9941.
[37] M.M.H. Khalil, E.H. Ismail, K.Z. El-Baghdady, D. Mohamed, Green synthesis of silver nanoparticles using olive leaf extract and its antibacterial activity, Arabian J. Chem 7 (2013) 1131–1139.
[38] A. Verma, M.S. Mehata, Controllable synthesis of silver nanoparticles using Neem leaves and their antimicrobial activity, J. Radiat. Res. Appl. Sci. 9 (2015) 109–115.
[39] Z. Sadowski, I.H. Maliszewska, B. Grochowalska, I. Polowczyk, T. Kozlecki, Synthesis of silver nanoparticles using microorganisms, Mater. Sci. Poland 26 (2008) 419–424.
[40] N. Kannan, S. Subbalaxmi, Biogenesis of nanoparticles—a current perspective, Rev. Adv. Mater. Sci. 27 (2011) 99–114.
[41] M. Dubey, S. Bhadauria, B.S. Kushwah, Green synthesis of nanosilver particles from extract of *Eucalyptus hybrida* (safeda) leaf, Dig. J. Nanomater. Biostruc. 4 (2009) 537–543.
[42] T.C. Prathna, A.M. Raichur, N. Chandrasekaran, A. Mukherjee, Heat mediated synthesis of silver nanoparticles using *Citrus limon* (Lemon) extract, Asian J. Chem. 25 (2013) S305–S307.
[43] J. Coates, Interpretation of infrared spectra, A practical approach, in: R.A. Meyers (Ed.), Encyclopedia of Analytical Chemistry, John Wiley & Sons Ltd, Chichester, 2000, pp. 10815–10837.
[44] M. Gajbhiye, J. Kesharwani, A. Ingle, A. Gade, M. Rai, Fungus-mediated synthesis of silver nanoparticles and their activity against pathogenic fungi in combination with fluconazole, Nanomed. Nanotechnol. Biol. Med. 5 (2009) 382–386.
[45] A. Barth, The infrared absorption of amino acid side chains, Prog. Biophys. Mol. Biol. 74 (2000) 141–173.
[46] B. Gole, C. Dash, V. Ramakrishnan, S.R. Sainkar, A.B. Mandale, M. Rao, M. Sastry, Pepsin-gold colloid conjugates: preparation characterization, and enzymatic, Langmuir 17 (2001) 1674–1679.
[47] H. Korbekandi, I. Siavash, Silver Nanoparticles, The delivery of nanoparticles, In: Dr. Abbass A. Hashim (Ed.), ISBN: 978-953-51-0615-9, (2012) InTech, 10.5772/34157.
[48] N. Ahmad, S., Sharma, V.N., Singh, S.F., Shamsi, A., Fatma, B.R. Mehta, Biosynthesis of silver nanoparticles from *Desmodium triflorum*: A novel approach towards weed utilization. Biotechnol. Res. Int. (2011) (Article ID 454090), 8 pages.
[49] N. Ahmad, S. Sharma, Green synthesis of silver nanoparticles using extracts of *Ananas comosus*, Green Sustainable Chem. 2 (2012) 141–147.
[50] D. Philip, C. Unni, S.A. Aromal, V.K. Vidhu, *Murraya koenigii* leaf-assisted rapid green synthesis of silver and gold nanoparticles, Spectrochim. Acta A 78 (2011) 899–904.
[51] B.G. Zanetti-Ramos, M.B. Fritzen-Garcia, C.S. de Oliveira, A.A. Pasa, V. Soldi, R. Borsali, T.B. Creczynski-Pasa, Dynamic light scattering and atomic force microscopy techniques for size determination of polyurethane nanoparticles, Mater. Sci. Eng. C 29 (2009) 638–640.
[52] V.A. Hackley, J.D. Clogston, Measuring the size of nanoparticles in aqueous media using batch-mode dynamic light scattering, NIST-NCL joint assay protocol PCC-1, Washington, D.C, 2007.
[53] N. Kovalchuk, V. Starova, P. Langston, N. Hilal, Formation of stable clusters in colloidal suspensions, Adv. Colloid Interfac. Sci. 147 (2009) 144–148.
[54] T. Schwede, J. Kopp, N. Guex, M.C. Peitsch, SWISS-MODEL: an automated protein homology-modeling server, Nucleic Acids Res. 31 (2003) 3381–3385.
[55] K. Arnold, L. Bordoli, J. Kopp, T. Schwede, The SWISS-MODEL Workspace: a web-based environment for protein structure homology modelling, Bioinformatics 22 (2006) 195–201.
[56] J.M. Panzner, M.S. Bilinovich, J.W. Youngs, C.T. Leeper, Silver metallation of hen egg white lysozyme: x-ray crystal structure and NMR studies, Chem. Commun. 47 (2011) 12479–12481.
[57] S.W. Kang, J.H. Kim, J. Won, K. Char, Y.S. Kang, Effect of amino acids in polymer/silver salt complex membranes on facilitated olefin transport, J. Membr. Sci. 248 (2005) 201–206.
[58] S. Erkoc, T. Yilmaz, Molecular-dynamics simulations of silver clusters, Physica E 5 (1999) 1–6.
[59] Z. Salari, F. Danafar, S. Dabaghi, S.A. Ataei, Sustainable synthesis of silver nanoparticles using macroalgae *Spirogyra varians* and analysis of their antibacterial activity, J. Chem. Saudi Chem. Soc. 20 (2016) 459–464.
[60] C.L. Keat, A. Aziz, A.M. Eid, N.A. Elmarzug, Biosynthesis of nanoparticles and silver nanoparticles, Bioresour. Bioprocess. 2 (2015) 1–11.
[61] S. Ahmed, M. Ahmad, B.L. Swami, S. Ikram, A review on plants extract mediated synthesis of silver nanoparticles for antimicrobial applications: a green expertise, J. Adv. Res. 7 (2016) 17–28.
[62] G. Rahimi, F. Alizadeh, A. Khodavandi, Mycosynthesis of silver nanoparticles from *Candida albicans* and its antibacterial activity against *Escherichia coli* and *Staphylococcus aureus*, Trop. J. Pharm. Res. 15 (2016) 371–375.
[63] A.R. Shahverdi, A. Fakhimi, H.R. Shahverdi, S. Minaian, Synthesis and effect of silver nanoparticles on the antibacterial activity of different antibiotics against *Staphylococcus aureus* and *Escherichia coli*, Nanomedicine 3 (2007) 168–171.
[64] I. Sondi, B. Salopek-Sondi, Silver nanoparticles as antimicrobial agent: a case study on *E. coli* as a model for Gram-negative bacteria, J. Colloid Interface Sci. 275 (2004) 177–182.
[65] A. Raja, S.M. Salique, P. Gajalakshmi, A. James, Antibacterial and hemolytic activity of green silver nanoparticles from *Catharanthus roseus*, Int. J. Pharm. Sci. Nanotechnol. 9 (2016) 3112–3117.
[66] J. Laloy, V. Minet, L. Alpan, F. Mullier, S. Beken, O. Toussaint, S. Lucas, D. Jean-Michel, Impact of silver nanoparticles on haemolysis: platelet function and coagulation, Nanobiomedicine 1 (2014) 1–9.
[67] L. Liu, J. Yang, J. Xie, Z. Luo, J. Jiang, Y.Y. Yang, S. Liu, The potent antimicrobial properties of cell penetrating peptide-conjugated silver nanoparticles with excellent selectivity for Gram-positive bacteria over erythrocytes, Nanoscale 5 (2013) 3834–3840.
[68] J. Choi, V. Reipa, V.M. Hitchins, P.L. Goering, R.A. Malinauskas, Physicochemical characterization and *in vitro* haemolysis evaluation of silver nanoparticles, Toxicol. Sci. 123 (2011) 133–143.
[69] C. Arulvasu, S.M. Jennifer, D. Prabhu, D. Chandhirasekar, Toxicity effect of silver nanoparticles in brine shrimp *Artemia*, Sci. World J. 2014 (2014) 1–10 (e256919).
[70] A. Phull, Q. Abbas, A. Ali, H. Raza, S.J. Kim, M. Zia, I. Haq, Antioxidant: cytotoxic and antimicrobial activities of green synthesized silver nanoparticles from crude extract of *Bergenia ciliata*, Future J. Pharm. Sci. 2 (2016) 31–36.